Int. J. Heat Mass Transfer. Vol. 25, No. 2, pp. 187–194, 1982
Printed in Great Britain

0017–9310/82/020187–08 $03.00/0
Pergamon Press Ltd.

THERMAL AND FLUID FLOW EFFECTS DURING SOLIDIFICATION IN A RECTANGULAR ENCLOSURE

N. RAMACHANDRAN*, J. P. GUPTA
Department of Chemical Engineering, Indian Institute of Technology Kanpur, Kanpur 208016, India

and

Y. JALURIA
Department of Mechanical Engineering, Indian Institute of Technology Kanpur, Kanpur 208016, India

(*Received* 25 *November* 1980 *and in revised form* 4 *April* 1981)

Abstract—An analysis is carried out for the solidification in a rectangular enclosure whose top and bottom surfaces are kept adiabatic and sides are kept at a constant temperature. The transient effects of solidification accompanied by natural convection have been studied in detail. The governing equations are written for the temperature, vorticity, stream function and velocity in the melt along with the heat conduction equations through the solid and the mold. The non-linear coupled equations have been non-dimensionalized and solved with the aid of the Alternating Direction Implicit finite difference method. The velocity profiles in the melt, and the temperature distribution in the melt, the solid and the mold are shown. Isotherms and streamlines in the melt are plotted for different Rayleigh numbers. The dependence of the melt–solid interface movement upon various non-dimensional parameters, such as Rayleigh number (5×10^2–5×10^5), Prandtl number (0.1–100), aspect ratio (1.1–5.5), Stefan number (0.5–10) and a parameter indicating the effect of superheat (0.67–2.33) are also studied.

NOMENCLATURE

C_p, specific heat [J/kg K];
d, thickness of the mold [m];
D, width of the enclosure [m];
g, gravitation constant [m/s^2];
Gr, Grashof number $= (g\beta(T_i - T_c)D^3/\nu^2)$;
k, thermal conductivity [J/s m K];
L, height of the enclosure [m];
L_q, latent heat of solidification [J/kg];
p, pressure [N/m^2];
Pr, Prandtl number $= \nu/\alpha$;
Ra, Rayleigh number $= Gr \cdot Pr$;
Ste, Stefan number $= L_q/C_p\,(T_i - T_c)$;
t, time [s];
t_n^*, present time level in finite difference form;
T, temperature [K];
T_c, mold outer surface temperature [K];
T_i, initial temperature [K];
T_{sat}, solidification temperature [K];
u, velocity in the x direction [m/s];
v, velocity in the y direction [m/s];
x, vertical coordinate measured from the bottom of the enclosure [m];
y, horizontal coordinate measured from the centre of the enclosure [m];
Y', half width of the melt region [m];
Y_0, distance from the centre line to solid–mold interface [m].

Greek symbols

α, thermal diffusivity [m^2/s];
β, temperature coefficient of cubical expansion [K^{-1}];
δ, relative width of melt region $= Y'/Y_0$;
ν, kinematic viscosity $= \mu/\rho$[m^2/s];
ϕ, dimensionless temperature $= (T_i - T_{sat})/(T_{sat} - T_c)$;
ρ, density [kg/m^3];
ψ, stream function [m^2/s];
ω, vorticity [s^{-1}].

Superscript

*, denotes dimensionless quantities.

Subscripts

l, melt;
m, mold;
s, solid.

INTRODUCTION

HEAT CONDUCTION problems with phase change have been studied extensively for over a century. These problems are encountered in a wide range of situations such as casting of metals and alloys, storage of thermal energy, spacecraft thermal protection design, freezing and thawing of foodstuffs etc. In modern foundary technology, the prediction of the solidification rate and the temperature distribution during the solidification process is very important in order to control the fundamental parameters, such as stripping time for static casting, and withdrawal rates for continuous casting, etc.

An examination of the available literature indicates that in most of the cases, the phase change problems

* Presently at the R&D Centre, Steel Authority of India Ltd., Ranchi, India.

have been treated as heat conduction problems. A series of analytical solutions have been reported in the literature, starting with the well known Stefan's problem. Cole [1] has examined the available literature and has given references of various analytical and numerical solutions available till 1969. In most of the investigations, the major emphasis is given to semi-infinite case or one dimensional heat conduction problems. The solidification of the melt in multi-dimensional enclosures of finite dimensions, for various boundary conditions has been discussed by Lazaridis [2] considering pure heat conduction.

However, the associated convective flow that is developed in the melt during solidification, has been given little attention so far. The natural convection flow developed in the melt due to thermal gradients is very important as it can have a large influence on the structure of the solid formed, apart from affecting the rate of solidification. In fact, they can even affect the distribution of the solutes in a multi-component system, which is so far believed to occur only by diffusion. Experimentally, the predominance of natural convection has been shown by Cole and Bolling [3]. The first attempt to study the convective flow quantitatively has been made by Szekely and Stanek [4] in their work on uni-directional solidification accompanied by natural convection. Ramachandran *et al.* [5] have solved the solidification problem with natural convection in a 1-dim. vertical slot for various boundary conditions, taking into account the heat conducted by the solid and the mold. Sparrow *et al.* [6] have made an elegant analysis of melting of a solid in a cylindrical enclosure, with the effect of natural convection in the melt. Experiments have been performed by Sparrow, Ramsey and Kemink [7] for the freezing of superheated and saturated melt in a cylindrical enclosure.

The present work was carried out to study solidification in a rectangular enclosure, taking into account the heat transfer in the melt, the solid formed and the mold containing them. The equations were solved for the adiabatic boundary condition at the top and the bottom of the enclosure, the mold walls being kept at a constant temperature. Velocity distribution, streamlines and isotherm patterns due to combined heat conduction and natural convection have also been obtained along with the interface movement with time.

ANALYSIS

Consider a rectangular enclosure of width $2Y_0$, mold thickness d and height L. The enclosure is extended to infinity in the z-direction, as shown in Fig. 1.

Initially, the mold is kept at a temperature T_c, which is less than the solidification temperature T_{sat}. At time $t = 0$, the melt at temperature T_i ($> T_{sat}$) is poured into the enclosure. Immediately, a thin crust of solid is formed adjacent to the inner surface of the mold, and an inward movement of the solid front starts. Because of the thermal gradients set up in the melt, a convection current starts in the melt.

In the analysis, the top and the bottom surfaces of the whole enclosure are kept adiabatic, while the outer vertical surfaces of the mold are kept at a constant temperature.

The following assumptions are made before writing the governing equations:

(i) The properties such as the density, thermal conductivity, specific heat etc. are assumed to be independent of temperature for the melt, the solid and the mold with the exception of the density of the melt which contributes to the buoyancy forces.

(ii) The fluid flow developed in the melt due to thermal gradients is assumed to be laminar.

(iii) The melt is assumed to be Newtonian.

(iv) The contact between the solid formed and the mold is assumed to be perfect, so that no contact resistance is introduced.

The equations are written for one half of the enclosure because of the symmetry at $y = 0$. We require the energy, momentum and continuity equations in the melt, and the energy equations in the solid and the mold, together with their initial and boundary conditions.

Thus, in the melt:

continuity equation:

$$\frac{\partial u}{\partial x} + \frac{\partial v}{\partial y} = 0; \tag{1}$$

momentum equations:

in the x direction

$$\frac{\partial u}{\partial t} + u\frac{\partial u}{\partial x} + v\frac{\partial u}{\partial y} = g\beta(T - T_{sat}) + \nu\left(\frac{\partial^2 u}{\partial x^2} + \frac{\partial^2 u}{\partial y^2}\right) - \frac{1}{\rho}\frac{\partial p}{\partial x} \tag{2}$$

and in the y direction

$$\frac{\partial v}{\partial t} + u\frac{\partial v}{\partial x} + v\frac{\partial v}{\partial y} = \nu\left(\frac{\partial^2 v}{\partial x^2} + \frac{\partial^2 v}{\partial y^2}\right) - \frac{1}{\rho}\frac{\partial p}{\partial y}; \tag{3}$$

energy equation:

$$\frac{\partial T_1}{\partial t} + u\frac{\partial T_1}{\partial x} + v\frac{\partial T_1}{\partial y} = \alpha_1\left(\frac{\partial^2 T_1}{\partial x^2} + \frac{\partial^2 T_1}{\partial y^2}\right). \tag{4}$$

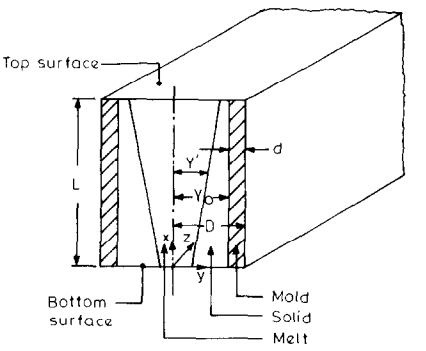

FIG. 1. Rectangular enclosure, infinite in z-direction.

The first term in the RHS of equation (2) is obtained via Boussinesq approximation [8] in which the density variation in the melt is considered only in so far as it contributes to buoyancy, otherwise it is neglected.

The problem can be simplified by combining equations (1)–(3), and writing in terms of vorticity ω and stream function ψ for ease in numerical computations.

Thus, the vorticity equation can be stated as

$$\frac{\partial \omega}{\partial t} + u\frac{\partial \omega}{\partial x} + v\frac{\partial \omega}{\partial y} = -g\beta\frac{\partial T}{\partial y} + \nu(\nabla^2\omega) \tag{5}$$

where

$$\omega = -\left(\frac{\partial^2\psi}{\partial x^2} + \frac{\partial^2\psi}{\partial y^2}\right), \tag{6}$$

$$u = \frac{\partial \psi}{\partial y}, \quad \text{and} \quad v = -\frac{\partial \psi}{\partial x}. \tag{7}$$

The energy equation in the solid is

$$\frac{\partial T_s}{\partial t} = \alpha_s\left(\frac{\partial^2 T_s}{\partial x^2} + \frac{\partial^2 T_s}{\partial y^2}\right), \tag{8}$$

and in the mold

$$\frac{\partial T_m}{\partial t} = \alpha_m\left(\frac{\partial^2 T_m}{\partial x^2} + \frac{\partial^2 T_m}{\partial y^2}\right). \tag{9}$$

The initial and the boundary conditions are:

in the melt:

$$\text{at } t = 0\text{: } T = T_i; \tag{10a}$$

$$\text{at } y = 0\text{: } \frac{\partial T_l}{\partial y} = 0; \quad \frac{\partial u}{\partial y} = 0; \; v = 0; \tag{10b}$$

$$\text{at } y = Y'\text{: } T = T_{sat}; \; u = 0; \; v = 0 \tag{10c}$$

and

$$\left(k_s\frac{\partial T_s}{\partial y} - k_l\frac{\partial T_l}{\partial y}\right)\left[1 + \left(\frac{\partial y'}{\partial x}\right)^2\right] = \rho L_q\frac{\partial y'}{\partial t}; \tag{10d}$$

at $x = 0$ and $x = L$:

$$\frac{\partial T_l}{\partial x} = 0; \quad u = 0 \text{ and } v = 0; \tag{10e}$$

in the solid:

$$\text{at } y = Y'\text{: } T_s = T_{sat}; \tag{11a}$$

$$\text{at } y = Y_0\text{: } T_s = T_m; \tag{11b}$$

$$\text{at } x = 0 \text{ and } x = L\text{: } \frac{\partial T_s}{\partial x} = 0; \tag{11c}$$

in the mold:

$$\text{at } t = 0\text{: } T_m = T_c; \tag{12a}$$

$$\text{at } y = Y_0\text{: } k_s\frac{\partial T_s}{\partial y} = k_m\frac{\partial T_m}{\partial y}; \tag{12b}$$

$$\text{at } t = 0\text{: } T_m = T_c; \; = \text{constant}; \tag{12c}$$

$$\text{at } x = 0 \text{ and } x = L\text{: } \frac{\partial T_m}{\partial x} = 0. \tag{12d}$$

To make the results more general, the following non-dimensional parameters are defined:

$$\left.\begin{aligned}
&x^* = x/L;\; y_l^* = y/Y'(t);\; t^* = \alpha_l t/D^2;\\
&u^* = \frac{uD^2}{\alpha_l L};\; v^* = \frac{vD}{\alpha_l};\; \psi^* = \frac{\psi D}{\alpha_l L};\\
&\omega^* = \omega D^3/\alpha_l L;\; T_l^* = (T_l - T_c)/(T_i - T_c);\\
&T_s^* = (T_s - T_c)/(T_i - T_c);\; y_s^* = \frac{y - Y'(t)}{Y_0 - Y'(t)};\\
&T_m^* = (T_m - T_c)/(T_i - T_c);
\end{aligned}\right\} \tag{13a}$$

$$Y_m^* = (y - Y_0)/(D - Y_0).$$

Because of the non-dimensionalization, the original variables, x, y, t are replaced by x^*, y^*, t^*. Thus,

$$\frac{\partial}{\partial t} = \frac{\alpha_l}{D^2}\frac{\partial}{\partial t^*} - \frac{y_l^*}{Y'}\frac{\partial Y'}{\partial t}\frac{\partial}{\partial y_l^*}, \tag{13b}$$

$$\frac{\partial}{\partial x} = \frac{1}{L}\frac{\partial}{\partial x^*} - \frac{y_l^*}{Y'}\frac{\partial Y'}{\partial x}\frac{\partial}{\partial y_l^*}, \tag{13c}$$

$$\frac{\partial}{\partial y} = \frac{1}{Y'}\frac{\partial}{\partial y_l^*}. \tag{13d}$$

In transforming equations (4)–(12), to equations (14)–(22) below, it has been assumed that the interface remains stationary for the period in which heat is extracted from it. During this period, the equations describing the fluid flow in the melt and the energy equations in the melt, the solid and the mold are solved assuming pseudo-steady state as discussed at great length by Sparrow *et al.* [6]. Because of this assumption the term $\partial Y'/\partial t$ appearing in the RHS of equation (13b) can be neglected. It has also been assumed that the thickness of the melt region Y' varies slowly with x so that the terms involving $\partial Y'/\partial x$, appearing in the RHS of equation (13c) is neglected. The inclusion of these terms would add significantly to the complexity and execution time of the numerical solutions. (Complete transformed equations including those terms are available in [9].) Sparrow *et al.* [6] have discussed that this assumption is quite valid as a first approximation in most cases of the phase change problems with natural convection.

Thus the transformed dimensionless equations are:

$$\frac{\partial T_l^*}{\partial t^*} = u^*\frac{\partial T_l^*}{\partial x^*} + v^*\left(\frac{D}{Y'}\right)\frac{\partial T_l^*}{\partial y_l^*} = \left(\frac{D}{L}\right)^2\frac{\partial^2 T_l^*}{\partial x^{*2}} + \left(\frac{D}{y'}\right)^2\frac{\partial^2 T_l^*}{\partial y_l^{*2}}, \tag{14}$$

$$\frac{\partial \omega^*}{\partial t^*} + u^*\frac{\partial \omega^*}{\partial x^*} + \left(\frac{D}{Y'}\right)v^*\frac{\partial \omega^*}{\partial y_l^*} = -\left(\frac{D}{L}\right)\left(\frac{D}{Y'}\right)\left(\frac{D}{Y_0}\right)^3 Ra \cdot Pr \cdot \frac{\partial T_l^*}{\partial y_l^*}$$

$$+\left(\frac{D}{L}\right)^2 Pr\frac{\partial^2\omega^*}{\partial x^{*2}}+\left(\frac{D}{Y'}\right)^2 Pr\frac{\partial^2\omega^*}{\partial y_1^{*2}}, \quad (15)$$

$$\omega^* = -\left(\frac{D}{L}\right)^2\frac{\partial^2\psi^*}{\partial x^{*2}}-\left(\frac{D}{Y'}\right)^2\frac{\partial^2\psi^*}{\partial y_1^{*2}}, \quad (16)$$

$$u^* = \left(\frac{D}{Y'}\right)\frac{\partial\psi^*}{\partial y_1^*}, \quad v^* = -\frac{\partial\psi^*}{\partial x^*}, \quad (17)$$

$$\frac{\partial T_s^*}{\partial t^*} = \frac{\alpha_s}{\alpha_l}\left[\left(\frac{D}{L}\right)^2\frac{\partial^2 T_s^*}{\partial x^{*2}}+\left(\frac{D}{Y_0-Y'}\right)^2\frac{\partial^2 T_s^*}{\partial y_s^{*2}}\right], \quad (18)$$

$$\frac{\partial T_m^*}{\partial t^*} = \frac{\alpha_m}{\alpha_l}\left[\left(\frac{D}{L}\right)^2\frac{\partial^2 T_m^*}{\partial x^{*2}}+\left(\frac{D}{D-Y_0}\right)^2\frac{\partial^2 T_m^*}{\partial y_m^{*2}}\right]. \quad (19)$$

The initial and the boundary conditions become:

in the melt:

$$\text{at } t^*=0:\ T_l^*=1; \quad (20a)$$

$$\text{at } y_l^*=0:\ \frac{\partial T_l^*}{\partial y_l^*}=0;\ \frac{\partial u^*}{\partial y_l^*}=0 \text{ and } v^*=0; \quad (20b)$$

$$\text{at } y_l^*=1:\ T_l^*=\frac{1}{(\phi+1)};\ u^*=0 \text{ and } v^*=0; \quad (20c)$$

$$\left[\frac{k_s}{k_l}\frac{1}{(1-\delta)}\frac{\partial T_s^*}{\partial y_s^*}-\frac{1}{\delta}\frac{\partial T_l^*}{\partial y_l^*}\right]\times\left[1+\left(\frac{Y_0}{L}\right)^2\left(\frac{d\delta}{dx^*}\right)^2\right]=Ste\left(\frac{Y_0}{D}\right)\frac{d\delta}{dt}; \quad (20d)$$

$$\text{at } x^*=0 \text{ and } x^*=1:\ \frac{\partial T_l^*}{\partial x^*}=0;\ u^*=0 \text{ and } v^*=0; \quad (20e)$$

in the solid:

$$\text{at } y_s^*=0:\ T_s^*=1/(\phi+1); \quad (21a)$$

$$\text{at } y_s^*=1:\ T_s^*=T_m^*; \quad (21b)$$

$$\text{at } x^*=0 \text{ and } 1:\ \frac{\partial T_s^*}{\partial x^*}=0; \quad (21c)$$

in the mold:

$$\text{at } t^*=0:\ T_m^*=0; \quad (22a)$$

$$\text{at } y_m^*=0:\ \frac{k_s}{k_m}\frac{\partial T_s^*}{\partial y_s^*}=\frac{Y_0-Y'}{D-Y_0}\frac{\partial T_m^*}{\partial y_m^*}; \quad (22b)$$

$$\text{at } y_m^*=1:\ T_m^*=0; \quad (22c)$$

$$\text{at } x^*=0 \text{ and } x^*=1:\ \frac{\partial T_m^*}{\partial y_m^*}=0. \quad (22d)$$

SOLUTION METHODOLOGY

Equations (14)–(22) were solved using finite difference technique and 10 × 10 spatial grids were established each for the melt, the solid and the mold. These grids were fine enough to resolve the steep temperature gradients near the interface at early times, for $Ra < 10^5$. More grids were provided for higher Rayleigh number to accommodate the rapid turning of the fluid near the interface. Grids were deployed non-uniformly similar to the grid system discussed by Spalding [10] for solving the boundary layer problems. The position of the interface was computed at the beginning of each time step using Chebyshev approximations [11]. In solving the moving interface equation (20d), the temperature gradients at the interface appearing in the equation were taken from the known values calculated through the previous time step. The energy equations for the melt, solid and the mold, and the vorticity equation for the melt were written in their central difference form and solved using the Alternating Direction Implicit (ADI) technique. The elliptic stream function equation (16) was solved using the Successive Over-Relaxation (SOR) method. The equations were solved sequentially.

At time $t^* = 0$, starting difficulties in the computation were avoided by assuming a very small thickness of the solid, due to chilling, equal to $0.0001\ Y_0$. It was also assumed that the temperature profile in the solid was linear at time $t^* = 0$ [12]. The initial thickness of the solid layer, due to chilling, was varied to ascertain that it did not influence the numerical solution. The tridiagonal matrices formed by the temperature and vorticity equations were solved using the general Tridiagonal Algorithm described by Roache [13]. Computations were made on a DEC-1090 computer.

RESULTS AND DISCUSSION

The temperature profiles in the melt, the solid and the mold at various heights, with non-dimensional time t^* as the parameter, are shown in Fig. 2. As the time progresses the temperature decays in the melt. The temperature of the melt is found to increase with the height, because of the natural convection developed in the melt. Initially, the temperature variation with the height of the enclosure is very little since conduction is dominating. Subsequently, natural convection currents are developed due to thermal gradients, which in turn take the hotter melt to the top of the enclosure driving the cooler melt towards the bottom.

The time dependent velocity profiles in the melt are shown in Fig. 3. The velocity profiles are symmetric about $y = 0$ and the net upward flow equals the net downward flow. With the progress in solidification, the vertical velocity of the melt increases, reaches a maximum value at some intermediate time and then decays. At time $t^* = 0.03$, the convection currents have just set in. The velocity near the top ($x/L = 0.9$) and near the bottom ($x/L = 0.1$) of the enclosure is found

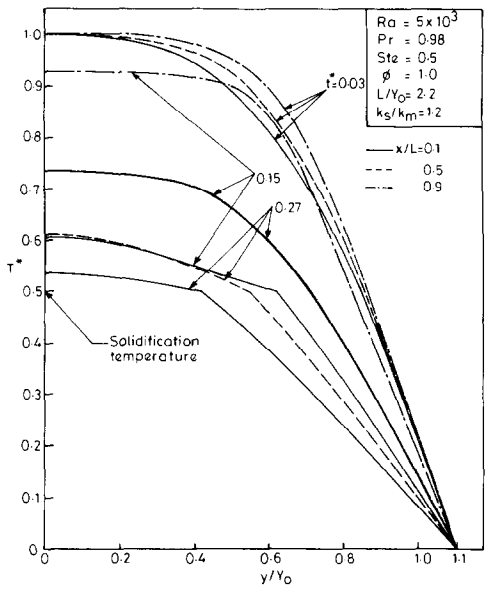

FIG. 2. Temperature profiles at different x/L.

to be the same, and the melt–solid interface is almost parallel to the wall. As the solidification progresses, the slope of the interface changes, and the velocity near the top becomes more than that near the bottom surface of the enclosure. A comparison of Figs. 2 and 3 at equal heights but different times indicates that the thermal field and the fluid motion decay almost at equal rates. This is true since $Pr = 0.98$, which suggests that the thermal and momentum diffusivities are nearly equal.

The streamlines and isotherms for the Rayleigh number 5×10^3 and at time $t^* = 0.27$ are shown in Figs. 4 and 5. It can be easily observed that the general characteristic of the flow pattern is upflow near the centre of the enclosure, where the melt is hotter and downflow near the melt–solid interface, where the melt

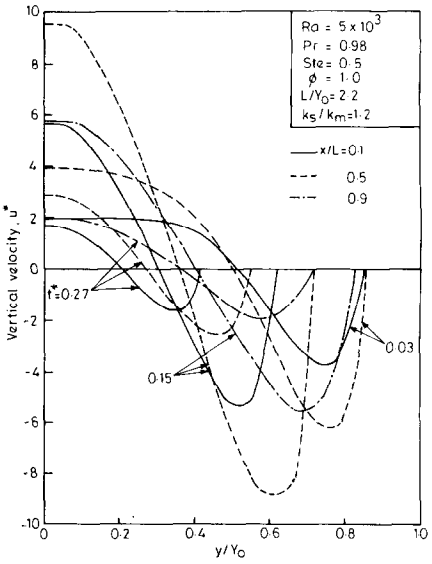

FIG. 3. Vertical velocity distribution in melt at different x/L.

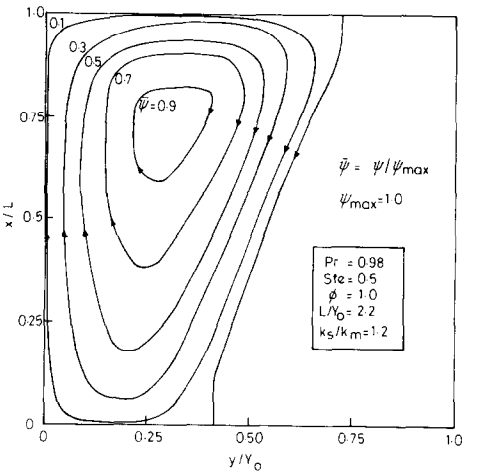

FIG. 4. Streamline patterns in melt for $Ra = 5 \times 10^3$ and $t^* = 0.27$.

is cooler. Both the streamlines and the isotherms indicate that at larger time, the thickness of the melt layer is greatest at the top and least at the bottom of the enclosure. It is interesting to note that the streamlines of higher values are restricted to the top portion of the enclosure, where the temperature and hence the flow is maximum. At high Rayleigh number ($Ra = 5 \times 10^5$) secondary cells are observed near the centre of the enclosure during the initial period of solidification as shown in Fig. 6.

An examination of Fig. 5 would indicate the predominance of the natural convection, where the isotherms are non-linear, contrary to the linear vertical isotherms one would expect in the case of pure conduction. Isotherms of higher values are concentrated near the centre of the top surface of the enclosure where the temperature is maximum.

The dependence of the interface movement on the Rayleigh number is shown in Fig. 7. At low Rayleigh number ($Ra = 5 \times 10^2$) where the natural convection is minimum, the shape of the interface is found to be

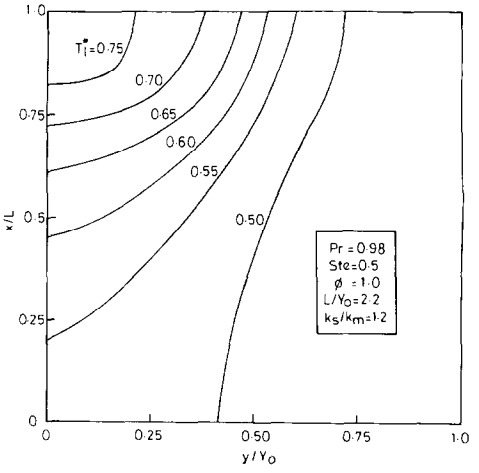

FIG. 5. Isotherm patterns in melt for $Ra = 5 \times 10^3$ and $t^* = 0.27$.

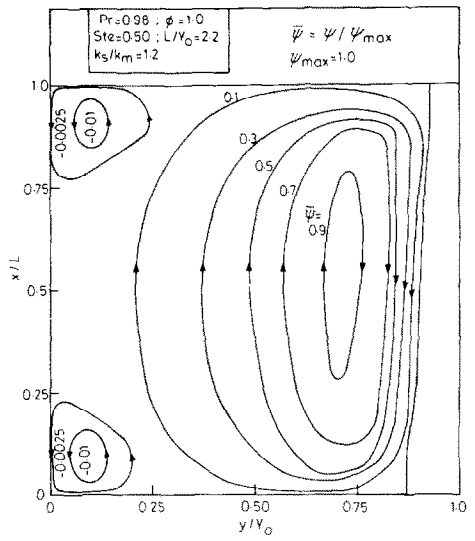

FIG. 6. Streamline patterns in melt for $Ra = 5 \times 10^6$ and $t^* = 0.03$.

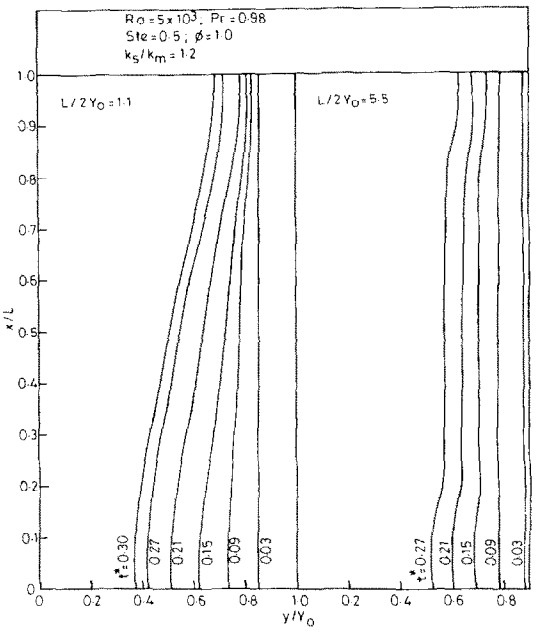

FIG. 8. Interface movement at different times for aspect ratios of 1.1 and 5.5.

almost vertical and parallel to the mold. As Ra approaches zero, the interface will be exactly vertical as conduction is the only mode of heat transfer. As Ra increases, heat transfer due to convection increases and the slope of the interface changes (Fig. 7). At low and moderate Rayleigh numbers the computation is carried up to non-dimensional time $t^* = 0.30$, whereas for high Rayleigh numbers, the computation is restricted to a time $t^* = 0.09$, due to enormous computation time required in the latter case.

The movement of the interface with time, for different aspect ratios ($L/2Y_0 = 1.1$ and 5.5) is shown in Fig. 8. At low aspect ratio, where the convection is maximum, the slope of the interface is high and it increases with time. At high aspect ratios, the interface is almost vertical except near the top and bottom of the enclosure, where the boundary effects start influencing the shape of the interface. This suggests that one can assume the heat transfer to be uni-directional when the aspect ratio is very high.

The influence of the Prandtl number (Pr) on the interface movement is shown in Fig. 9. As Pr increases the interface slope increases up to $Pr = 10$. Interestingly Prandtl number greater than 10 does not have any influence on the interface movement, and an

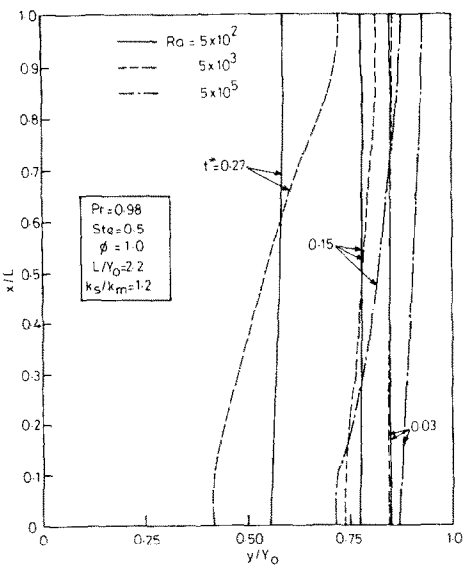

FIG. 7. Dependence of interface movement upon Rayleigh number at different times.

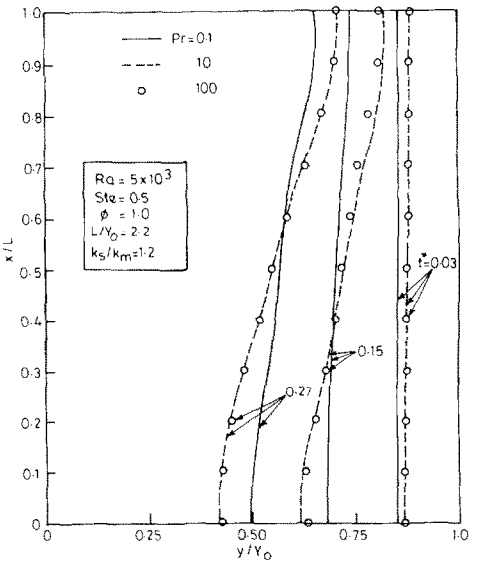

FIG. 9. Dependence of interface movement upon Prandtl number at different times.

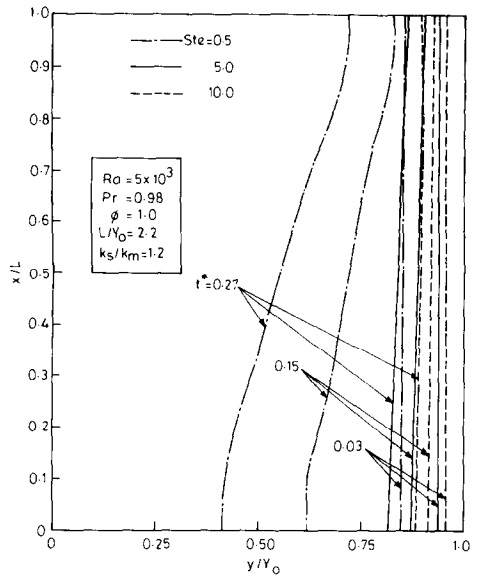

FIG. 10. Dependence of interface movement upon Stefan number at different times.

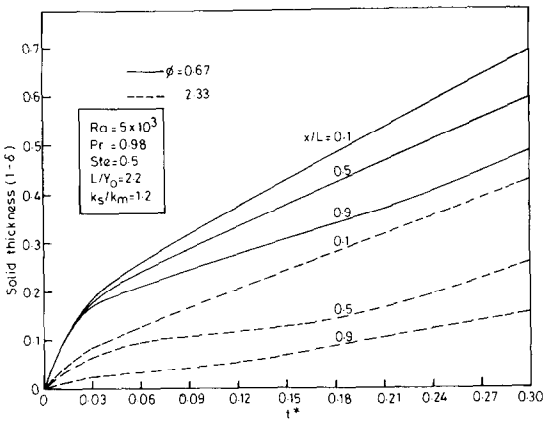

FIG. 11. Effect of superheat on thickness of the solid formed.

asymptotic solution is reached. This is evident from equation (15) which suggests that the vorticity does not change with time at high Prandtl numbers. This supports the results discussed by Sparrow *et al.* [6].

The effect of the Stefan number (*Ste*) on the rate of interface movement is shown Fig. 10. The melt–solid interface is found to proceed faster when *Ste* is small, as expected.

The dependence of the solidification rate on the superheat (ϕ) can be understood from Fig. 11, where the thickness of the solid formed is plotted with time, with ϕ as the parameter. It can be seen from Fig. 11 that the rate of movement of solid front decreases with increase in ϕ. This is expected since large ϕ implies higher value of superheat and hence a decrease in the solidification rate.

CONCLUDING REMARKS

An analysis has been carried out for the solidification in a rectangular enclosure. The equations were written for the temperature, vorticity, stream function and velocities in the melt. Consideration has also been given to the heat conducted through the solid formed and the mold. The coupled, non-linear, simultaneous equations have been solved using the ADI finite difference technique. The thickness of the solid formed at every time step has been found by solving the energy balance equation at the melt–solid interface.

The temperature and velocity profiles are plotted at various heights in the enclosure. The temperature is found to increase with the height. It has also been found that the natural convection has significant effect on the shape of the interface. The vertical velocity component and the temperature decay at almost equal rates when the Prandtl number is close to unity. The effect of natural convection on solidification is clearly shown in the isotherm and streamlines plotted for different Rayleigh numbers. Finally, the rate of solidification is also studied for various non-dimensional parameters such as the Rayleigh number, Prandtl number, aspect ratio, Stefan number and the extent of superheat.

Acknowledgement—One of the authors (N. R.) wishes to acknowledge his thanks to the R & D Centre for Iron and Steel, Sail, Ranchi, India for sponsoring his work on this project.

REFERENCES

1. G. S. Cole, Solidification, Paper presented at the Seminar of Am. Soc. for Metals, p. 201. American Society for Metals, Metals Park, Ohio (1969).
2. A. Lazaridis, A numerical solution of the multidimensional solidification (or melting) problem, *Int. J. Heat Mass Transfer* **13**, 1459–1477 (1970).
3. G. S. Cole and G. F. Bolling, The importance of natural convection in casting, *Trans. TMS-AIME* **233**, 1568 1572 (1965).
4. J. Szekely and V. Stanek, Natural convection transients and their effects in unidirectional solidification, *Metall. Trans.* **1**, 2243–2251 (1970).
5. N. Ramachandran, Y. Jaluria and J. P. Gupta, Thermal and fluid flow characteristics in one-dimensional solidification, *Lett. Heat Mass Transfer* **8**, 69–77 (1981).
6. E. M. Sparrow, S. V. Patankar and S. Ramadhyani, Analysis of melting in the presence of natural convection in the melt region, *Trans. A.S.M.E., J. Heat Transfer* **99**, 520–526 (1977).
7. E. M. Sparrow, J. W. Ramsey and R. G. Kemink, freezing controlled by natural convection, *Trans. A.S.M.E., J. Heat Transfer*, **101**, 578–584 (1979).
8. Y. Jaluria, *Natural Convection Heat and Mass Transfer*. Pergamon Press, Oxford, U.K. (1980).
9. N. Ramachandran, A study of solidification in an enclosed region with natural convection in the melt. Ph.D. thesis submitted to Chemical Engineering Department, Indian Institute of Technology, Kanpur (1981).
10. D. B. Spalding, *GENMIX—A General Computer Program For Two-Dimensional Parabolic Phenomena*. Pergamon Press, Oxford, U.K. (1977).
11. B. Carnahan, H. A. Luther and J. O. Wilkes, *Applied Numerical Methods*. Wiley, New York, U.S.A. (1969).
12. H. Schlichting (Ed.) *Boundary Layer Theory* Vol. 6. McGraw–Hill, New York, U.S.A. (1969).
13. P. J. Roache, *Computational Fluid Dynamics*. Hermosa, Albuquerque, New Mexico, U.S.A. (1976).

EFFETS THERMIQUES ET DYNAMIQUES PENDANT LA SOLIDIFICATION D'UN FLUIDE DANS UNE CAVITE RECTANGULAIRE

Résumé—On analyse la solidification dans une cavité rectangulaire dont les surfaces supérieure et inférieure sont adiabatiques tandis que les côtés sont maintenus à température constante. On étudie en détail la solidification accompagnée par la convection naturelle. Les équations fondamentales sont écrites pour la température, la vorticité, la fonction de courant et la vitesse dans le bain avec les équations de la conduction thermique dans le solide et le bain. Les équations couplées non-linéaires sont rendues sans dimension et résolues à l'aide d'une méthode implicite aux différences finies et avec directions alternées. Les profils de vitesse dans le bain sont donnés ainsi que la distribution de température dans le bain et dans le solide. Des isothermes et des lignes de courant dans le bain sont tracées pour différents nombres de Rayleigh. On étudie aussi la dépendance du mouvement à l'interface bain-solide vis-à-vis des paramètres adimensionnels tels que le nombre de Rayleigh (5×10^2–5×10^5), le nombre de Prandtl (0,1–100), le rapport de forme (1,1–5,5), le nombre de Stefan (0.5–10) et un paramètre indiquant l'effet de surchauffe (0,67–2,33).

THERMISCHE UND STRÖMUNGSBEDINGTE VORGÄNGE WÄHREND DER ERSTARRUNG IN EINEM RECHTECKIGEN GESCHLOSSENEN BEHÄLTER

Zusammenfassung—Es wurde eine Untersuchung über die Erstarrung in einem rechteckigen geschlossenen Raum durchgeführt, dessen Ober- und Unterseite adiabat sind und dessen Seiten auf einer konstanten Temperatur gehalten werden. Die zeitlichen Vorgänge der Erstarrung, die von freier Konvektion begleitet sind, wurden detailliert untersucht. Die beschreibenden Gleichungen berücksichtigen Temperatur, Wirbeligkeit, Stromfunktion und Geschwindigkeit in der Schmelze sowie die Wärmeleitung in der erstarrten Phase und in der Form. Die nichtlinearen gekoppelten Gleichungen wurden dimensionslos gemacht und mit Hilfe des impliziten finiten Differenzenverfahrens der alternierenden Richtungen (ADI-Verfahren) gelöst. Es werden die Geschwindigkeitsprofile in der Schmelze und die Temperaturverteilung in der Schmelze, der festen Phase und in der Form angegeben. Für verschiedene Rayleigh-Zahlen sind die Isothermen und Stromlinien in der Schmelze grafisch dargestellt. Ferner wurde die Abhängigkeit der Bewegung der Erstarrungsgrenze von verschiedenen dimensionslosen Parametern wie Rayleigh-Zahl ($5 \cdot 10^2$–$5 \cdot 10^5$), Prandtl-Zahl (0,1–100), Seitenverhältnis (1,1–5,5), Stefan-Zahl (0,5–10) und einem Parameter, der den Einfluß der Überhitzung beschreibt (0,67–2,33), untersucht.

ТЕПЛОВЫЕ И ГИДРОДИНАМИЧЕСКИЕ ЭФФЕКТЫ ПРИ ЗАТВЕРДЕВАНИИ ЖИДКОСТИ В ПРЯМОУГОЛЬНОЙ ПОЛОСТИ

Аннотация — Проведен анализ процесса затвердевания в прямоугольной полости, верхняя и нижняя поверхности которой являются адиабатическими, а боковые имеют постоянную температуру. Подробно исследуется нестационарный процесс затвердевания, сопровождающийся естественной конвекцией. Для определения температуры, степени завихренности, функции тока и скорости жидкости в расплаве выведены основные уравнения наряду с уравнениями передачи тепла теплопроводностью через твердое тело и прессформу. Нелинейные сопряженные уравнения приведены к безразмерному виду и решены неявным конечно-разностным методом переменных направлений. Представлены профили скорости в расплаве и распределения температур в расплаве, твердом теле и прессформе. Построены изотермы и линии тока в расплаве при различных значениях числа Релея. Исследована также зависимость движения границы раздела «расплав-твердое тело» от различных безразмерных параметров, таких как число Релея ($5 \cdot 10^2$–$5 \cdot 10^5$), число Прандтля (0,1–100), отношение сторон (1,1–5,5), число Стефана (0,5–10) и параметра, учитывающего влияние перегрева (0,67–2,33).